

## The Parkfield, California, Earthquake Prediction Experiment

W. H. Bakun and A. G. Lindh

Certain sections of the San Andreas fault system in central California tend to fail in recurring, moderate-sized (magnitude 5 to 7), characteristic earthquakes (1, 2). Characteristic earthquakes are repeat earthquakes that have the same faulting mechanism, magnitude, rupture length, location, and, in some cases, the same epicenter and direction of rupture propagation as earlier shocks. The earthquakes in 1979 at Coyote Lake and in 1984 at Morgan Hill, both of magnitude 6 (Fig. 1, inset), on the southern Calaveras fault east of San Jose, California, are recent examples of characteristic earthquakes, apparently repeating shocks in 1897 and 1911, respectively (3, 4). The case for characteristic earthquakes on the Parkfield section of the San Andreas fault (Fig. 1) is more complete (5), at least in part because the interval between events at Parkfield is shorter (21 to 22 years) than the interval (70 to 85 years) that is apparently appropriate for the southern Calaveras fault (3, 4).

In recent years, earthquakes near Parkfield (Fig. 1) have occurred either on the San Andreas fault or in distinct clusters of activity near the western edge of the San Joaquin Valley (6). Northwest of the Parkfield section, slip on the San Andreas fault occurs predominantly as aseismic fault creep; although small shocks (magnitude <4) occur here frequently, shocks of magnitude 6 and larger are unknown and little, if any, strain is accumulating (7). In contrast, very few microearthquakes and no aseismic slip have been observed on the fault southeast of Cholame; this locked section ap-

parently ruptures exclusively in large earthquakes (magnitude >7), most recently during the great Fort Tejon earthquake of 1857 (8). Parkfield earthquakes occur within the transition zone between these contrasting modes of fault failure. The regular nature of Parkfield seismicity since 1857 may be due to the nearly

---

**Summary.** Five moderate (magnitude 6) earthquakes with similar features have occurred on the Parkfield section of the San Andreas fault in central California since 1857. The next moderate Parkfield earthquake is expected to occur before 1993. The Parkfield prediction experiment is designed to monitor the details of the final stages of the earthquake preparation process; observations and reports of seismicity and aseismic slip associated with the last moderate Parkfield earthquake in 1966 constitute much of the basis of the design of the experiment.

---

constant slip rate pattern on the adjoining sections of fault. Until recently, the Parkfield section had been relatively free of significant perturbations in stress caused by nearby shocks; the effect of the 2 May 1983 Coalinga earthquake [local magnitude ( $M_L$ ) 6.7], 40 km northeast of Parkfield (Fig. 1), on the timing of the next Parkfield shock is not known.

### Historic Parkfield Seismicity

The epicenters of two foreshocks of magnitude 6 in 1857, as well as the epicenter of the 1857 main shock, were probably located on the San Andreas fault near Parkfield (9). Since 1857, earthquake sequences with main shocks of magnitude 6 have occurred near Parkfield on 2 February 1881, 3 March 1901, 10 March 1922, 8 June 1934, and 28 June 1966. The times between sequences since 1857 are remarkably uniform, with

a mean interval of  $21.9 \pm 3.1$  (standard deviation of the mean) years (Fig. 2b). Although the time of the 1934 sequence departs from the regular pattern by occurring a decade too early, the time of the 1966 sequence conforms to the regular pattern, in that the 44 years between 1922 and 1966 is twice the mean interval.

The last damaging Parkfield earthquake in 1966 was assigned a value for  $M_L$  of 5.6 (5, 10) and a seismic moment of  $1.4 \times 10^{25}$  dyne-cm (11). Although the shock might have caused significant damage if it had occurred in a metropolitan area, it caused only minor damage to the wooden frame homes in the sparsely populated Parkfield region (12, 13). The source of the 1966 earthquake can be described by a simple model: unilateral rupture propagation southeast over the rupture zone, a 20- to 25-km-long section of the San Andreas fault bounded by two

geometric discontinuities in the fault trace that apparently control the extent of rupture (14). The northwest discontinuity, adjacent to the epicenter of the 1966 main shock on Middle Mountain, is a 5° change in the strike of the fault trace; the southeast discontinuity is a 1-km echelon offset (right step) in the fault trace near Gold Hill. The Parkfield preparation zone is the 1- to 2-km-long section of fault at the northwest end of the rupture zone; the preparation zone is defined to include the 5° bend in the fault trace and the epicenters of the 1966 main shock and its foreshock ( $M_L$  5.1) (Fig. 1).

### The Characteristic Parkfield Earthquake

The 1934 and 1966 Parkfield sequences were remarkably similar (5, 10). The main shocks had identical epicenters, magnitudes, fault-plane solutions, and unilateral southeastward ruptures.

The authors are with the Department of the Interior, Geological Survey, Branch of Seismology, 345 Middlefield Road, Menlo Park, California 94025.

Moreover, identical foreshocks of  $M_L$  5.1 preceded each main shock by 17 minutes (10), and the lateral extent of aftershock epicenters in 1966 (15) repeated that in 1934 (16). The location and extent of surface faulting in 1934 were similar to those in 1966, and anecdotal reports suggest that, after the 1922 and 1901 events, cracks were found in some of the same places as well (12). Intensity patterns for the Parkfield shocks in 1901, 1922, 1934, and 1966 are similar (9); the few reports available for the 1881 Parkfield shock (17) are consistent with the intensities reported for the more recent shocks. The epicentral location of the main shock in 1922 is constrained to the 18-km-long section of the fault northwest of the rupture zone (18). Comparisons of

seismograms for the 1922, 1934, and 1966 main shocks recorded in Europe, North America, and South America suggest that, within the experimental errors of 10 to 20 percent, the seismic moments for the three shocks were equal (5).

Although few data are available for Parkfield sequences before 1934, they are consistent with the proposal that the main shocks in 1881, 1901, and 1922 were similar to those in 1934 and 1966 (5). The similarities in the main shocks (19) suggest that the Parkfield section of the San Andreas fault is characterized by recurring earthquakes with predictable features. Thus, the design of a prediction experiment can be tailored to the specific features of the recurring characteristic earthquake.

## A Recurrence Model for Parkfield Earthquakes

The limited data available on the recurrence of large and great earthquakes along plate boundaries around the world apparently are consistent with a time-predictable model, for which the time interval between successive shocks is proportional to the coseismic displacement of the preceding earthquake (20, 21). Unfortunately this simple model is not supported by the data available for the last three Parkfield earthquakes: although comparable coseismic displacements in 1922, 1934, and 1966 are inferred from the observations (5), the time intervals between the three events differ by more than a factor of 2 [1934 to 1922 (12 years) compared with 1966 to 1934 (32 years)].

However, simple adjustments result in another model, the Parkfield recurrence model, which partially accounts for the timing of the characteristic Parkfield shocks (see Fig. 2a). Both models assume a constant loading rate and an upper bound stress threshold,  $\sigma_1$ , corresponding to the failure strength, or yield stress, of the fault. Whereas the time-predictable model permits a variable stress drop, the Parkfield recurrence model assumes the same stress drop for each characteristic earthquake but allows for the possibility of an occasional early failure, that is, before  $\sigma_1$  is reached. The Parkfield recurrence model implies that the stress drop in a characteristic earthquake generally does not completely relieve stress in the rupture zone.

The features of the Parkfield recurrence model are easily described. Failure at or near  $\sigma_1$  corresponds to those times when the failure stress is approached over the entire rupture zone, at which time failure must occur; according to this model there can be no late characteristic Parkfield earthquakes. However, triggering scenarios (22) can be devised that permit the occasional early characteristic earthquake.

There may be evidence for an early triggering mechanism in the seismicity preceding the 1934 event. The foreshocks during the 3 days before the main shock in 1934 were initiated by a cluster of magnitude 3 events and a subsequent shock of  $M_L$  5.0 (23). This early  $M_L$  5 foreshock, which occurred 55 hours before the 1934 main event and about 3 km northwest (16), was characterized by unilateral rupture expansion southeast toward the preparation zone (24), a particularly efficient mechanism for increasing right-lateral shear stress in the prepa-

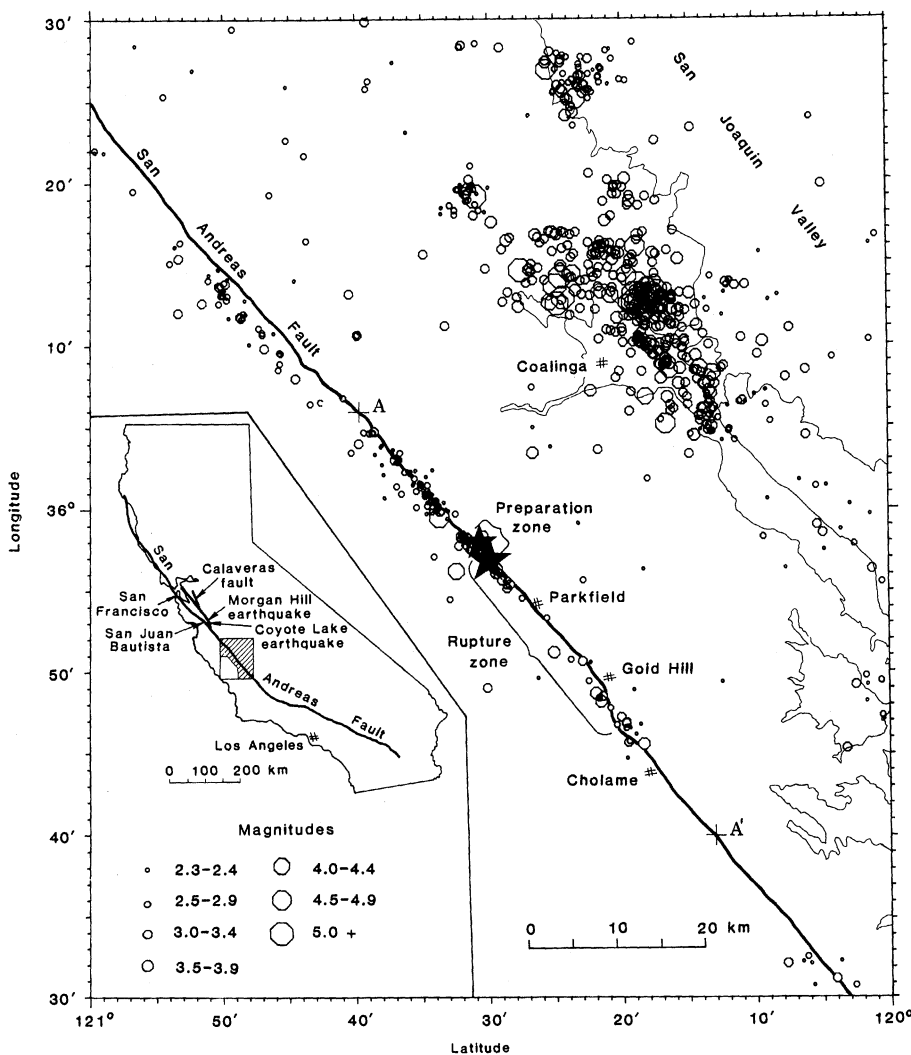


Fig. 1. Map of earthquake epicenters (1975-1984) relative to the trace of the San Andreas fault (bold line) and the epicenters of the foreshock ( $M_L$  5.1) and the main shock in 1966 (small and large stars, respectively, near the center of the map). All epicenters were calculated from a crustal velocity model designed specifically for the Parkfield section of the San Andreas fault (55). Brackets along the fault show the preparation zone and rupture zone of characteristic Parkfield earthquakes. Epicenter clusters near the western edge (faint line) of the San Joaquin Valley are aftershocks of the earthquakes at Cantua Creek in 1975, at Avenal in 1976, at New Idria in 1982, and at Coalinga in 1983. Epicenters for all earthquakes of  $M_L$  2.3 or greater are shown, except the very many aftershocks ( $M_L < 3$ ) of the 1983 Coalinga earthquake, which cover the Coalinga area when plotted.

ration zone. This early foreshock may have triggered the failure within the preparation zone, including the immediate foreshock of  $M_L$  5.1 and the main shock (25).

The Parkfield area was relatively quiet for shocks of  $M_L$  4 or greater in the years following the 1934 and 1966 sequences (Fig. 2c); more active periods began in 1953 and 1975. This pattern is reminiscent of the seismic cycle modulations in regional seismicity that accompany great plate-boundary earthquakes (26). Perhaps there is an intermediate stress level,  $\sigma_2$ , reached midway in the recurrence cycle (27), at which moderate seismicity ( $M \geq 4$ ) resumes in the Parkfield area. The 1934 Parkfield sequence occurred approximately when  $\sigma_2$  would have been reached (Fig. 2). We can speculate that, while the early foreshock in 1934 should have just marked the onset of the active half of the seismic cycle, it triggered a sequence of shocks near the preparation zone that culminated in the immediate foreshock and the 1934 characteristic earthquake.

According to the model, the next characteristic Parkfield earthquake should occur before  $\sigma_1$  is exceeded (early 1988 from Fig. 2). The uncertainty in this predicted time can be estimated from the regression of times of characteristic earthquakes that we presume occurred at  $\sigma_1$  (28). From the relation  $T_O = 21.7I + 1836.2$  (line in Fig. 2b), where  $T_O$  is the time of origin (in years) and  $I$  is a characteristic earthquake counter (5), the 95 percent confidence interval for the predicted date is  $1988.0 \pm 5.2$  (29). That is, the next characteristic Parkfield earthquake should occur before 1993.

### Recent Seismicity

The significant recent seismic activity on the San Andreas fault near Parkfield is concentrated near the ends of the 1966 rupture zone (Figs. 1 and 3), the same spatial pattern that preceded the 1979 Coyote Lake and 1984 Morgan Hill earthquakes (3, 30). Seismic activity on the creeping section northwest of the preparation zone is characterized by shallow focal depths and a small average magnitude, which are typical features of seismicity along the creeping section of the fault northwest to San Juan Bautista (31). The recent seismicity within the rupture zone mimics the spatial and magnitude distributions of the 1966 aftershocks (32), even though the events shown in Figs. 1 and 3 occurred well after the end of the 1966 aftershock ac-

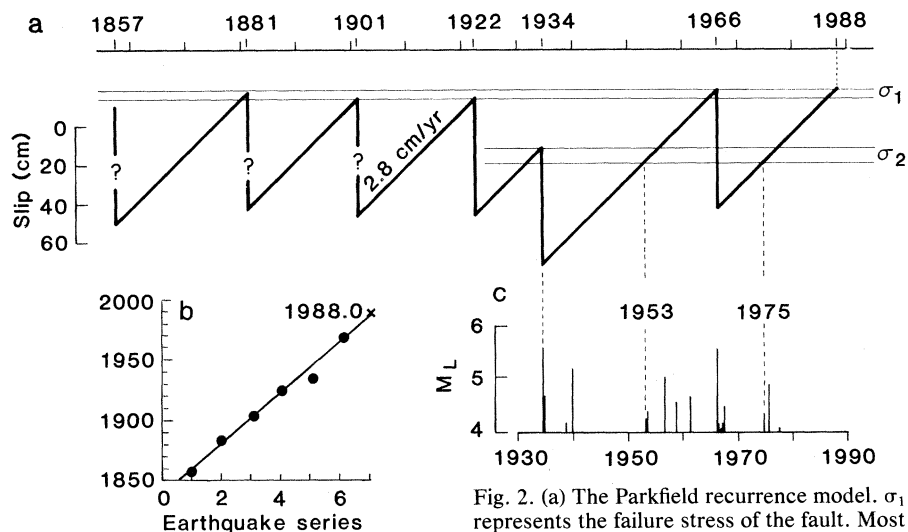


Fig. 2. (a) The Parkfield recurrence model.  $\sigma_1$  represents the failure stress of the fault. Most characteristic earthquakes occur at  $\sigma_1$ ; the 1934 shock occurred at  $\sigma_2$ . A constant loading rate of 2.8 cm per year and a coseismic slip of 60 m for the Parkfield earthquake sequences in 1881, 1901, 1922, 1934, and 1966 are assumed (56). (b) Series of earthquake sequences at Parkfield since 1850 [after (5)]. The line represents the linear regression of the time of the sequence obtained without the 1934 sequence. The anticipated time of the seventh (that is, the next) Parkfield sequence for the regression is January 1988. (c) Shocks of  $M_L$  greater than 4 since 1930 have tended to occur when the stress exceeds  $\sigma_2$ .

tivity (33). Apparently, the distribution of seismicity within the rupture zone is controlled by relatively stationary fault zone properties, such as geometry (30, 34) or rock type (35).

The seismic activity near the preparation zone (36) is most critical for short-term earthquake prediction. All but one of the  $M \geq 4$  shocks in the Parkfield area since 1969 have occurred within 1 to 2 km of the preparation zone. On 13 September 1975, a shock of  $M_L$  4.9 with low static stress drop (24) occurred 5 km northwest of the preparation zone; rupture propagated southeast, apparently stopping near the preparation zone. This shock appears to be similar in many respects to the early foreshock in 1934 (and to the shock of  $M_L$  5 on 16 November 1956) (24), but it did not trigger an early characteristic earthquake, although it did initiate the current active phase of the seismic cycle (Fig. 2c). Since 1975, a number of clusters of magnitude 3 shocks, the most recent in June 1982, have occurred near the preparation zone.

The static stress drops of the immediate foreshocks of  $M_L$  5.1 in 1934 and 1966 were marginally higher than those of other shocks of  $M_L$  5 located near, but not within, the preparation zone (24). Higher static stress drops were also obtained for a set of recent smaller shocks located close to the preparation zone; sources of lower stress drop tend to occur around the sources of higher stress drop (37). Perhaps the preparation zone is characterized by sources of relatively

high stress drop, whether or not the earthquakes are foreshocks.

Signals from seismographs (38) near Parkfield (Fig. 4) are telemetered continuously to a central data-processing facility in Menlo Park, California. The signals are automatically and continuously monitored by a real-time processor (39) that, within a few minutes, routinely locates earthquakes in central California. Beeper and paging systems have been established so that the responsible scientists are notified within minutes of all significant seismicity near the preparation zone.

### Crustal Deformation

An irrigation pipeline that crosses the rupture zone 2 km northwest of Gold Hill broke and separated about 9 hours before the 1966 Parkfield main shock (40). Also, fresh en echelon cracks of uncertain origin were observed in the fault zone near the center of the rupture zone 12 days before the 1966 earthquake; if the cracks were tectonic, they resulted from aseismic slip in the rupture zone (41). An optimistic interpretation of the broken pipeline and the fresh cracks is that a few centimeters or more of precursory fault creep occurred in the rupture zone just before the 1966 earthquake. Although these observations are fragmentary, and although subsequent earthquakes elsewhere in California have not produced any further evidence for premonitory slip, laboratory observations

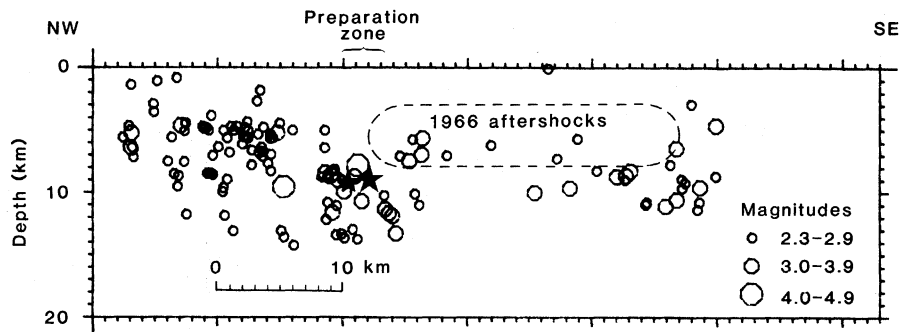


Fig. 3. Cross section of the seismicity for 1975-1984 along the section A-A' (Fig. 1) of the San Andreas fault. Relative focal depths are generally accurate to 1 km or less; depths of the shallow shocks northwest of the preparation zone are less accurate, with an uncertainty of about 2 km. For reference, the hypocenters of the immediate foreshock of  $M_L$  5.1 and the main shock in 1966 are shown as small and large stars, respectively, and the approximate outline of the 1966 aftershock zone (rupture zone) is dashed.

and theoretical calculations (42) indicate that premonitory deformation should occur near the hypocenter, although the amount and timing are uncertain. In light of the crucial importance of this question for future directions in earthquake prediction research, a major effort has been undertaken at Parkfield to define whatever premonitory deformation precedes the next earthquake there.

On a more fundamental basis, the deformation measurements define the tectonic framework within which all the Parkfield observations must be interpreted. The Parkfield section of the San Andreas fault is a relatively simple part of the North American-Pacific plate boundary, with no major active intersecting faults nearby. Below 10 to 20 km, the relative motion of the Pacific and North American plates apparently occurs as steady right-lateral slip at about 3.5 cm per year (43). Relative plate motion on the San Andreas fault at shallower depths is accommodated by infrequent great earthquakes southeast of Cholame and by aseismic slip or small

shocks (or both) northwest of the preparation zone; the transition occurs near Parkfield (44).

Within this context, the Parkfield rupture zone is an asperity, or "stuck patch," on the fault plane approximately 5 km wide; that is, it extends 3 to 8 km in depth and about 25 km in length. This patch is being loaded by slipping portions of the fault northwest of and beneath it, and is either completely "stuck" between earthquakes, or is slipping, but at a rate much slower than the loading rate of 3.5 cm per year. As such, it is an analog for large plate-boundary earthquakes on transform faults, which typically involve widths of 10 to 20 km and lengths of 100 km and greater. Thus, the Parkfield experiment is most significant in that earthquakes here are apparently large enough to embody the essential features of a great plate-boundary earthquake. There is a period of strain accumulation (in this case, about 20 years) when slip within the rupture zone is less than the rate of relative plate motion. This period is followed by the

sudden slip in the earthquake when the rupture zone "catches up." The details of the crustal deformation preceding the next Parkfield earthquake should lead to a clearer understanding of the strain accumulation and release process at a plate boundary and thus should guide our efforts to predict great plate-boundary earthquakes elsewhere.

Efforts to monitor deformation at Parkfield address two specific questions:

1) Will the strain release during the next earthquake be approximately the inverse, both in amount and distribution, of the strain accumulation since the 1966 shock? The answer is crucial to the basic assumptions underlying earthquake recurrence models, such as the time-predictable and Parkfield recurrence models, which are the foundation of long-term prediction efforts.

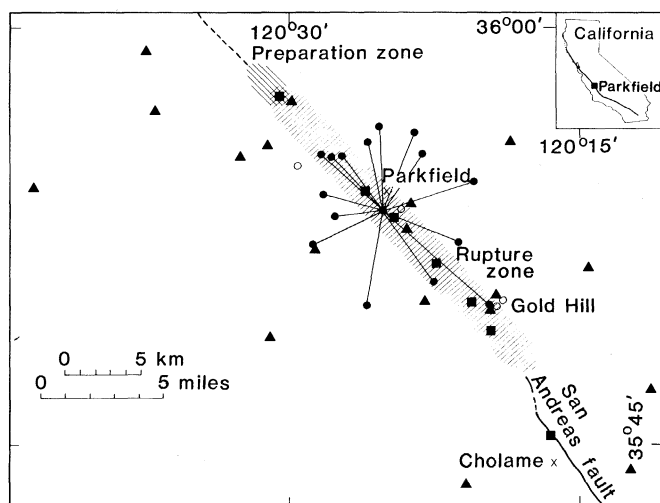
2) Are there changes in the details of the deformation field that might permit a refined estimate of the time of the next earthquake? The answer to this question will have a major impact on efforts toward medium- and short-term prediction.

Because of their importance, these questions are addressed by several projects to monitor deformation near Parkfield. A dense geodetic network with line lengths of 5 to 30 km spanning the fault has been measured every 1 to 2 years since 1969; the lengths are measured to a precision of 0.3 to 0.5 part per million, so that these data should establish the average slip during the next earthquake to an accuracy of better than 10 percent (45). Because of the inherent difficulties of resolving slip at depth and the uncertain time scale of the strain accumulation process, details of the deformation changes are perhaps better resolved by other techniques.

Lengths of lines spanning the rupture zone (Fig. 4) are measured several times each week with a two-color laser distance-measuring device that is capable of resolving length changes of about 1 mm over the 5- to 8-km-long lines (46). These observations should provide some additional resolution of the long-term deformation, but more important, they should resolve details of the deformation within the rupture zone during the days to months before the next earthquake.

While the geodetic observations are relatively insensitive to long-term systematic errors, they are difficult to measure frequently. In efforts to overcome this limitation and to improve the sensitivity to short-term changes, borehole volumetric strainmeters (47) are being installed in the Parkfield area (Fig. 4). These dilatometers provide continuous

Fig. 4. Seismometers ( $\blacktriangle$ ), borehole dilatometers ( $\circ$ ), creepmeters ( $\blacksquare$ ), and lines of the geodetic figure monitored with two-color laser ( $\bullet$ ) near the preparation and rupture zones of Parkfield characteristic earthquakes.



data with a sensitivity of about 1 part per billion over periods of a few hours. The resolution of these data overlaps the resolution of the two-color laser measurements for periods of a few weeks and is one to two orders of magnitude more sensitive at shorter periods.

In addition, a number of low-sensitivity 10- to 20-m-long wire strainmeters (creepmeters) span the surface trace of the San Andreas fault near Parkfield (Fig. 4). These creepmeters can detect a few millimeters of anomalous fault slip and are well suited to detect premonitory slip of the magnitude that may have occurred in 1966. However, interpretation of fault creep measurements along the San Andreas fault is complicated by the effects of the Coalinga earthquake ( $M_L$  6.7) of 2 May 1983. Not only was the character of creepmeter recordings along a 40-km-long section of the San Andreas fault strongly affected by the Coalinga earthquake (48), but an unusual swarm of small shocks 18 km southeast of Cholame on the locked section of the San Andreas fault occurred a few days after the Coalinga main shock (49).

#### A Larger Shock

It is possible that the next characteristic Parkfield earthquake might break through the en echelon offset at the southeast end of the rupture zone and continue southeast along the San Andreas fault, growing into a major earthquake. Alternatively, the characteristic earthquake might stop at the en echelon offset and, by analogy to the triggering mechanism of the early foreshock of  $M_L$  5.0 in 1934, increase the right-lateral shear stress on the fault southeast of the rupture zone. The latter case has been suggested (9) as the triggering mechanism for the great Fort Tejon earthquake of 1857.

Slip in 1857 along the 50-km-long section of the San Andreas fault southeast of Cholame was about 3.5 m, appreciably less than the 9-m offset farther southeast (50). Continuation of a Parkfield earthquake southeast might result in a rupture length of about 90 km, which is consistent with a magnitude 6.5 to 7 earthquake (2). Since the average Holocene offset rate across the San Andreas fault at Wallace Creek is 3.5 cm per year (51), it seems likely that the 3.5 m of slip in 1857 has largely been recovered, so that the possibility of an earthquake breaking this segment must be taken seriously. There are few data available to suggest what precursors there might be for this hypothetical larger shock. Minor

differences in the stress field near the offset, the strength of the offset, and the dynamic stress ahead of the rupture could all be important (52). Although foreshocks or deformation (or both) at the southeast end of the Parkfield rupture zone might portend a shock significantly larger than a characteristic Parkfield earthquake, there is certainly no evidence that such precursors need occur.

#### Discussion

Experiments in predicting the detailed characteristics of the source of a significant earthquake, such as the next Parkfield earthquake, provide opportunities for many kinds of investigations. In addition to the elements of the prediction experiment, geophysical instrumentation is being deployed near Parkfield that will take advantage of the predicted features of the coming earthquake to address specific outstanding issues of earthquake mechanics. For example, a network of nearly 50 strong-motion accelerographs operated by the California Division of Mines and Geology near the Parkfield rupture zone is designed to provide a direct measure of the velocity of rupture, estimates of the history and amplitude of the seismic slip along the rupture length, detailed information about high-frequency radiation and directivity effects, and a test of the idea that the low-rigidity fault zone might act as a wave guide that significantly distorts seismic radiation (53).

Two fundamentally different models of the earthquake generation process have been used in our description of the phenomena at Parkfield. The propagating crack models (type 1) derived from analyses of seismograms feature discontinuous slip beginning at a point (the hypocenter) and expanding over the rupture surface (54). For these type 1 models, precursory aseismic slip is generally not considered, precursors are expected near the epicenter (the preparation zone), and the preparation zone is viewed as a relatively strong point on the fault surface. The evidence for larger stress drops for earthquakes within the Parkfield preparation zone would support the type 1 models. However, laboratory experiments in rock mechanics (42) suggest that stick-slip events—the earthquake analog in rock mechanics—are always preceded by stable sliding—the fault creep analog in rock mechanics. These observations have been used in support of strain-softening models (type 2) of the earthquake generation process

(42). For these type 2 models, at least some precursory aseismic slip is required near the hypocenter; zones of precursory aseismic slip might have significant lateral extent, perhaps extending beyond the preparation zone. For the type 2 models, earthquake precursors should be concentrated near the relatively weak places on the fault surface where the aseismic slip occurs. The anecdotal reports of the broken irrigation pipeline and the en echelon cracks observed before the 1966 Parkfield earthquake are qualitative evidence supporting the type 2 strain-softening models of the earthquake generation process. The evaluation of these two different types of models, implicit in the design of the Parkfield prediction experiment, is essential before focused efforts to record short-term precursors can be undertaken in other earthquake-prone areas.

#### References and Notes

1. A. G. Lindh, *U.S. Geol. Surv. Open-File Rep.* 83-63 (1983).
2. L. R. Sykes and S. P. Nishenko, *J. Geophys. Res.* **89**, 5905 (1984).
3. W. H. Bakun *et al.*, *Science* **225**, 288 (1984).
4. P. Reasenber and W. L. Ellsworth, *J. Geophys. Res.* **87**, 10637 (1982).
5. W. H. Bakun and T. V. McEvilly, *ibid.* **89**, 3051 (1984).
6. The 1982 New Idria sequence (main shock  $M_L$  5.4) and the 1983 Coalinga sequence (main shock  $M_L$  6.7) shown in Fig. 1 are examples of the seismic activity associated with the development of the prominent fold structures between the San Andreas fault and the San Joaquin Valley [see J. Eaton, R. Cockerham, F. Lester, *Calif. Div. Mines Geol. Spec. Publ.* 66, 261 (1983)].
7. J. C. Savage and R. O. Burford, *J. Geophys. Res.* **76**, 6469 (1971).
8. C. R. Allen, *Stanford Univ. Publ. Geol. Sci.* **11**, 70 (1968).
9. K. E. Sieh, *Bull. Seismol. Soc. Am.* **68**, 1731 (1978).
10. W. H. Bakun and T. V. McEvilly, *Science* **205**, 1375 (1979).
11. Y. B. Tsai and K. Aki, *Bull. Seismol. Soc. Am.* **59**, 275 (1969).
12. R. D. Brown, Jr., J. G. Vedder, R. E. Wallace, E. F. Roth, R. F. Yerkes, R. O. Castle, A. O. Waananan, R. W. Page, J. P. Eaton, *U.S. Geol. Surv. Prof. Pap.* 579 (1967).
13. C. A. von Hake and W. K. Cloud, *United States Earthquakes, 1966* (U.S. Coast and Geodetic Survey, Washington, D.C., 1968).
14. A. G. Lindh and D. M. Boore, *Bull. Seismol. Soc. Am.* **71**, 95 (1981).
15. T. V. McEvilly, W. H. Bakun, K. B. Casaday, *ibid.* **57**, 1221 (1967).
16. J. T. Wilson, *ibid.* **26**, 189 (1936).
17. T. R. Toppozada, C. R. Real, D. L. Parke, *Calif. Div. Mines Geol. Open-File Rep.* 81-11 SAC (1981).
18. The data permit a common epicenter for the 1922, 1934, and 1966 main shocks near the southeast end of the preparation zone (5). There are no seismograms that might constrain the epicenter locations of the 1881 and 1901 shocks.
19. Although the features of the main shocks are similar, there are notable differences in the foreshock activity. The 1934 main shock was preceded by a nearly 3-day-long foreshock sequence, including a foreshock ( $M_L$  5.0) 55 hours before the main shock (16). Although the immediate (17 minutes before) foreshocks of  $M_L$  5.1 in 1934 and 1966 were identical (10), early foreshock activity comparable to that in 1934 did not occur in 1966. There are no reports of felt foreshocks preceding the main shocks in 1881, 1901, or 1922, so that foreshocks of  $M_L$  5 probably did not precede these characteristic shocks. Furthermore, no foreshocks in 1922 are evident on the Bosch-Omori seismograms written at Berkeley; shocks of  $M_L$  4.5 near Parkfield probably would be noticeable on these records.
20. K. Shimazaki and T. Nakata, *Geophys. Res.*

- Lett.* 7, 279 (1980); L. R. Sykes and R. C. Quittmeyer, *Am. Geophys. Union Monogr. Earthquake Prediction*, 217 (1981).
21. The fundamental principles of the time-predictable model are well established [H. F. Reid, *The California Earthquake of April 18, 1906* (Carnegie Institution of Washington, Washington, D.C., 1910), part 2]. That is, an earthquake occurs when the strain accumulated since the preceding earthquake results in sufficient stress to rupture the fault surface. Adding the concepts of a constant failure stress threshold, a constant rate of strain accumulation, and variable stress drop results in the time-predictable model.
  22. J. N. Brune, *J. Geophys. Res.* 84, 2195 (1979).
  23. G. S. Buhr and A. G. Lindh, *U.S. Geol. Surv. Open-File Rep.* 82-205 (1982); W. H. Bakun and A. G. Lindh, *Earthquake Pred. Res.*, in press.
  24. W. H. Bakun and T. V. McEvilly, *Bull. Seismol. Soc. Am.* 71, 423 (1981).
  25. While the foreshock cluster may have provided the immediate triggering mechanism, the conditions that permitted this to occur only in 1934 are not resolved. Accelerated loading rate associated with nonuniform regional strain accumulation [W. Thatcher, *Nature (London)* 299, 12 (1982)], accelerated fault creep near the preparation zone, temporal changes in the fault strength associated with fluctuations in pore pressure, and so forth could have contributed. Such "out of sequence" events may simply be statistical fluctuations resulting from the nonlinear interaction of a large number of factors, such as an ensemble of asperities in the preparation zone, each obeying a somewhat different strain-softening constitutive law.
  26. D. Tocher, *Calif. Div. Mines Geol. Spec. Rep.* 57, 39 (1959); S. A. Fedetov, in *Seismic Zoning of the U.S.S.R.*, S. Medvedev, Ed. (U.S.S.R. Academy of Science, Moscow, 1968).
  27. K. Mogi, *Am. Geophys. Union Monogr. Earthquake Prediction*, 43 (1981).
  28. The 1934 time, corresponding to  $\sigma_2$  rather than  $\sigma_1$ , was not used in these calculations. Although the details of seismicity at Parkfield in 1857 are uncertain, the 1857 date is used since we presume that it represents failure at  $\sigma_1$  (Fig. 2).
  29. The standard error in the estimated origin time (given the sequence counter) is 1.2 years [W. J. Dixon and F. J. Massey, Jr., *Introduction to Statistical Analyses* (McGraw-Hill, New York, 1957)]. The significance of the 95 percent confidence interval calculation is extremely limited given the small sample size (3 degrees of freedom) and the apparent inconsistency of the Gaussian assumption. An analysis of long-term probabilities ( $I$ ) yields an estimate of 67 percent probability of a characteristic Parkfield earthquake by the spring of 1993 (1988.0 + 5.2 years). The corresponding Poisson expectation,  $1 - \exp(-8.2/21.9)$ , is 31 percent.
  30. W. H. Bakun, *Bull. Seismol. Soc. Am.* 70, 1181 (1980).
  31. The abrupt termination of this shallow seismicity, about 6 km northwest of the preparation zone, coincides with the southeast limit of the contact of Franciscan melange with the San Andreas fault trace. For 150 km northwest, the creeping section is associated with Franciscan melange east of the fault; no melange material outcrops farther southeast, and the surface creep decreases to zero near Cholame.
  32. J. P. Eaton, M. E. O'Neill, J. N. Murdock, *Bull. Seismol. Soc. Am.* 60, 1161 (1970).
  33. All shocks of  $M_L$  4 or greater and most of  $M_L$  between 3 and 4 occur within the two distinct clusters at 8 to 10 km depth at the two ends of the 1966 aftershock zone, similar to the results obtained for late aftershocks in 1966 (32).
  34. W. H. Bakun *et al.*, *Bull. Seismol. Soc. Am.* 70, 185 (1980).
  35. Although there is little basement outcrop adjoining the rupture zone northeast of the San Andreas fault, there are slivers of granite and crystalline metamorphic rocks on Middle Mountain and a large outcrop of gabbro near Gold Hill, suggesting that the basement adjacent to the rupture zone is of higher density, and possibly higher strength, than the Franciscan melange rocks that adjoin the creeping section to the northwest (31).
  36. The locations for the two 1966 shocks are relative to precise hypocentral locations for several of the largest shocks near the preparation zone since 1975; epicenter and focal depth precisions are 1 km and 2 km, respectively.
  37. M. E. O'Neill, *Bull. Seismol. Soc. Am.* 74, 27 (1984).
  38. Telemetered, high-gain, short-period seismic stations in the U.S. Geological Survey's central California seismic network have operated continuously in the Parkfield region since April 1969. The network has expanded from a small regional network of 4 single-component vertical stations to a comprehensive network of 14 high-gain, short-period vertical stations and 8 3-component stations with improved dynamic range. The 14 high-gain vertical stations are being upgraded with improved dynamic range instruments, and data transmission is being transferred from long-distance, dedicated phone lines to a microwave telemetry system.
  39. R. A. Allen, *Bull. Seismol. Soc. Am.* 68, 1521 (1978).
  40. The broken irrigation pipeline has been attributed to 1 to 2 feet of southeast movement of the northeast end relative to the southwest end (12), consistent with right-lateral strike-slip displacement across the fault. However, the history of the movement is unknown, so that perhaps only a small part occurred in the days and weeks just before the 1966 earthquake.
  41. The discovery of these cracks in June 1966 (12) led to a 24-hour microearthquake survey of the area on 18 and 19 June 1966, 8 days before the main shock; no identifiable shocks of  $M_L$  1 or greater occurred within a distance of 24 km [C. R. Allen and S. W. Smith, *Bull. Seismol. Soc. Am.* 56, 966 (1966)]. Seismograms at Gold Hill showed that no shocks of  $M_L$  1 or greater occurred within the rupture zone in the 6 days before the 1966 main shock and that only six occurred in the preceding 5.5 months [G. Buhr, G. Matooka, A. Lindh, M. Frosenbaugh, *Earthquake Notes* 49 (No. 4), 41 (1978)]. This level of seismicity is about 15 percent of the average seismicity level within the rupture zone; the significance of this relative quiescence is difficult to assess in light of the clustered nature of the recent seismicity.
  42. J. H. Dieterich, *J. Geophys. Res.* 83, 3940 (1978); J. R. Rice, *Gerlands Beitr. Geophys.* 88, 91 (1979); W. D. Stuart, R. J. Archuleta, A. G. Lindh, *J. Geophys. Res.* 90, 592 (1985); S. T. Tse, R. Dmowska, J. R. Rice, *Bull. Seismol. Soc. Am.* 75, 709 (1985).
  43. W. Thatcher, *J. Geophys. Res.* 84, 2283 (1979).
  44. Surface slip rates since 1966 are 3.0 to 3.5 cm per year to the northwest, 2 cm per year above the preparation zone, less than 1 cm per year near Gold Hill, and 0 southeast of Cholame [M. Lisowski and W. H. Prescott, *Bull. Seismol. Soc. Am.* 71, 1607 (1981)]. Whereas nearly continuous aseismic surface slip (fault creep) is common to the northwest, creep within the rupture zone tends to be episodic, with events of up to a few millimeters of slip occurring in a few hours [S. S. Schulz *et al.*, *J. Geophys. Res.* 87, 6977 (1982)]. Creep events apparently extend down less than 1 km, propagating to the surface over a few days [N. R. Gouly and R. Gilman, *J. Geophys. Res.* 83, 5415 (1978)].
  45. W. F. Slawson and J. C. Savage, *Bull. Seismol. Soc. Am.* 73, 1407 (1983).
  46. The two-color laser is a prototype instrument operated in cooperation with L. Slater of the University of Colorado. Noise levels on a similar array near Hollister, California, were  $10^{-7}$  to  $2 \times 10^{-7}$  strain [J. O. Langbein *et al.*, *Science* 218, 1217 (1982)].
  47. The Sacks-Evertson volumetric strainmeter (or borehole dilatometer) measures changes in pressure within a fluid-filled cylinder cemented in place at depths of 100 to 500 m [I. S. Sacks, S. Suyehiro, D. W. Evertson, *Proc. Jpn. Acad.* 47, 707 (1971)]. These instruments are an important component of earthquake prediction efforts in Japan [K. Mogi, *Am. Geophys. Union Monogr. Earthquake Prediction*, 635 (1981)].
  48. The maximum calculated stress change along the San Andreas fault was not more than about 1 bar [G. M. Mavko, S. Schulz, B. D. Brown, *Bull. Seismol. Soc. Am.* 75, 475 (1985)]. Nevertheless, the pattern of fault creep recorded by the Middle Mountain creepmeter located atop the Parkfield preparation zone was drastically altered. Left lateral slip occurred from 2 May 1983 to mid-August 1984, when the normal right-lateral movement resumed [S. S. Schulz, G. M. Mavko, B. D. Brown, *U.S. Geol. Surv. Prof. Pap.*, in press].
  49. W. L. Ellsworth *et al.*, *Eos* 64, 749 (1983). Earlier moderate shocks east of the San Andreas fault were also followed by small shocks on the San Andreas fault north of Simmler: a magnitude 2.9 shock occurred 32 days after the Avenal earthquake ( $M_L$  4.7) of 14 January 1976 and a magnitude 2.1 shock occurred 2 days after the New Idria earthquake ( $M_L$  5.4) of 25 October 1982.
  50. K. E. Sieh, *Bull. Seismol. Soc. Am.* 68, 1421 (1978).
  51. K. E. Sieh and R. H. Jahns, *Geol. Soc. Am. Bull.* 95, 883 (1984).
  52. S. Das and K. Aki, *J. Geophys. Res.* 82, 5658 (1977).
  53. R. D. McJunkin and A. F. Shakal, *Calif. Geol.* 36, 27 (1983).
  54. See, for example, N. A. Haskell, *Bull. Seismol. Soc. Am.* 54, 1811 (1964); J. N. Brune, *J. Geophys. Res.* 75, 4997 (1970); R. Madariaga, *Bull. Seismol. Soc. Am.* 66, 639 (1976).
  55. R. Nowack, unpublished data. Epicenters not near Parkfield are less accurate.
  56. Right-lateral plate motion of 29 mm per year was obtained (43) in an inversion of geodetic measurements near the creeping section of the San Andreas fault northwest of Parkfield. For slip between 3 and 8 km depth and a rupture length of 25 km, coseismic slip in 1966 was 60 cm (14).
  57. We thank J. Dieterich, W. Ellsworth, A. McGarr, R. Page, and J. Savage for comments on the manuscript, K. Poley for her help with the data analysis and preparation of the figures, and the people of the Parkfield area for their generous cooperation, interest, and friendship. Without their help this experiment would not have been possible.